nature biotechnology

# A reversibly photoswitchable GFP-like protein with fluorescence excitation decoupled from switching

Tanja Brakemann[1,6], Andre C Stiel[1,6], Gert Weber[2], Martin Andresen[1], Ilaria Testa[1], Tim Grotjohann[1], Marcel Leutenegger[1], Uwe Plessmann[3], Henning Urlaub[3,4], Christian Eggeling[1], Markus C Wahl[2], Stefan W Hell[1] & Stefan Jakobs[1,5]

**Photoswitchable fluorescent proteins have enabled new approaches for imaging cells, but their utility has been limited either because they cannot be switched repeatedly or because the wavelengths for switching and fluorescence imaging are strictly coupled. We report a bright, monomeric, reversibly photoswitchable variant of GFP, Dreiklang, whose fluorescence excitation spectrum is decoupled from that for optical switching. Reversible on-and-off switching in living cells is accomplished at illumination wavelengths of ~365 nm and ~405 nm, respectively, whereas fluorescence is elicited at ~515 nm. Mass spectrometry and high-resolution crystallographic analysis of the same protein crystal in the photoswitched on- and off-states demonstrate that switching is based on a reversible hydration/dehydration reaction that modifies the chromophore. The switching properties of Dreiklang enable far-field fluorescence nanoscopy in living mammalian cells using both a coordinate-targeted and a stochastic single molecule switching approach.**



Fluorescent proteins (FPs)[1] whose fluorescence can be reversibly or irreversibly switched by optical irradiation have opened new opportunities for the imaging of cells. They have facilitated *in vivo* protein-tracking schemes[2,3], applications based on single-molecule observations[4,5] and fluorescence microscopy with subdiffraction resolution[6–10].

Still, photoswitchable proteins have not displayed their full potential, because proteins that are just photoactivatable[11–13] can be switched only once, which implies that repeated measurements with the same molecule are impossible. On the other hand, photochromic or reversibly switchable fluorescent proteins (RSFPs) can be repeatedly photoswitched between a fluorescent and a nonfluorescent state by irradiation with light of two different wavelengths. However, in all previously characterized RSFPs, the wavelength used for generating the fluorescence emission is identical to one of the wavelengths used for switching the fluorescence on or off. The result is a complex interlocking of switching and fluorescence readout[14–22], impeding or even precluding many applications, including fluorescence nanoscopy (super-resolution microscopy). Hence, the identification of an RSFP in which the generation of fluorescence is disentangled from switching has long been pursued.

## RESULTS

### Generation of the RSFP Dreiklang

Numerous GFP variants exhibit some degree of (generally undesirable) reversible photoswitching[4,23,24]. We found that the fluorescence of the yellow fluorescent protein Citrine[25,26], a derivative of GFP, can be reversibly modulated to a small extent by alternate irradiation with light of 365 nm (on switching) and 405 nm (off switching), whereas fluorescence is excited at 515 nm. However, the achievable contrast was low, especially at pH values >6, rendering the reversible switching of Citrine unusable (**Supplementary Fig. 1**).

To further develop this unusual switching behavior, we performed extensive random mutagenesis as well as directed PCR-mediated mutagenesis on a plasmid encoding Citrine. We transformed *Escherichia coli* with the plasmid, and screened with an automated home-built fluorescence microscope for bacterial colonies expressing fluorescent proteins whose fluorescence was excited with green light (515 nm) and which could be reversibly photoswitched from a fluorescent state to a long-lived nonfluorescent state by irradiation with near-UV (405 nm) light and back to a fluorescent state by UV (365 nm) light (**Fig. 1a**). In several consecutive screening rounds ~70,000 individual clones were analyzed. Finally, we identified a mutant differing from Citrine at four positions (Citrine-V61L, F64I, Y145H, N146D) (**Supplementary Fig. 2**), which can be effectively switched and excited to fluoresce. We named this switchable fluorescent protein Dreiklang, the German word for a three-note chord in music.

At thermal equilibrium, Dreiklang adopts the brightly fluorescent on-state, with a quantum yield of 0.41 and an extinction coefficient of 83,000 $M^{-1}cm^{-1}$ at pH 7.5 (**Table 1**). In the on-state, it exhibits two absorption bands (peaking at 412 nm and 511 nm), corresponding to the neutral (protonated) and ionized (deprotonated) states of the chromophore, respectively (**Fig. 1b**)[1]. The $pK_a$ of the on-state chromophore is 7.2, which is 1.5 pH units higher than the $pK_a$ of

[1]Max Planck Institute for Biophysical Chemistry, Department of NanoBiophotonics, Göttingen, Germany. [2]Freie Universität Berlin, Institut für Chemie und Biochemie, AG Strukturbiochemie, Berlin, Germany. [3]Max Planck Institute for Biophysical Chemistry, Bioanalytical Mass Spectrometry, Göttingen, Germany. [4]University Medical Center Göttingen, Department of Clinical Chemistry, Bioanalytics, Göttingen, Germany. [5]University of Göttingen Medical School, Göttingen, Germany. [6]These authors contributed equally to this work. Correspondence should be addressed to S.W.H. (shell@gwdg.de) or S.J. (sjakobs@gwdg.de).

Received 12 April; accepted 20 July; published online 11 September 2011; doi:10.1038/nbt.1952

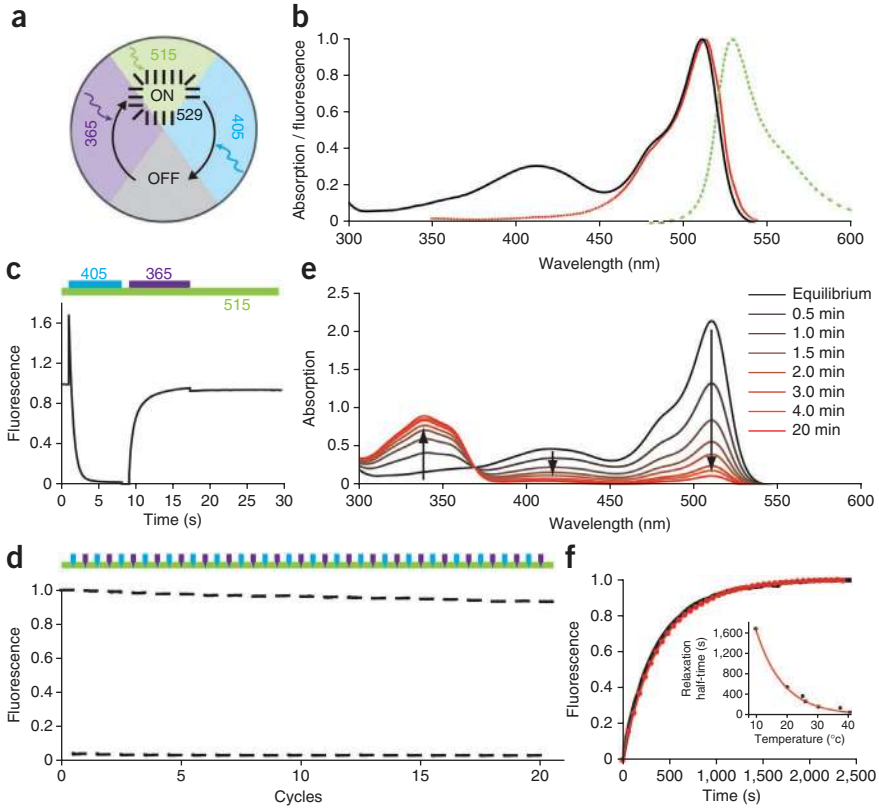


**Figure 1** Properties of Dreiklang. (**a**) Scheme depicting Dreiklang's switching modality. (**b**) Normalized absorbance (solid black line), fluorescence emission (dashed green line) and fluorescence excitation (dotted red line) spectra of the (fluorescent) equilibrium-state Dreiklang at pH 7.5. (**c**,**d**) Switching curves of Dreiklang's fluorescence recorded on colonies of living *E. coli*. Off- and on-switching was performed with near-UV (405 nm) and UV light (365 nm), respectively, and fluorescence read-out with green light (515 nm). The respective irradiation scheme is indicated on top of the graphs by the colored bars. (**c**) One switching cycle. Fluorescence was continuously recorded. (**d**) Twenty consecutive switching cycles. Fluorescence was recorded when the cells were irradiated with green light only. (**e**) Irradiation-dependent changes in Dreiklang absorbance. Absorbance spectra obtained at the indicated time points during switching of equilibrium-state Dreiklang (pH 7.5) into the off-state by irradiation with 405 nm. (**f**) Irradiation-independent changes in Dreiklang fluorescence due to the thermal equilibration from the off-state into the fluorescent equilibrium state. After off-switching, fluorescence was recorded at 25 °C under constant irradiation with 515 nm (black line) or by consecutive 20-ms pulses of 515 nm light in 60 s intervals (red dots). The similar curves demonstrate that 515 nm light does not photoswitch Dreiklang. Inset: relaxation half-time from the off- into the equilibrium-state as a function of temperature. The data were obtained on purified Dreiklang (pH 7.5) (circles) or on living cells expressing Dreiklang targeted to the ER (squares). Red line: single exponential fit to the data obtained on purified protein.



Citrine (5.7) (**Supplementary Fig. 1c**,**d**)[26]. Hence, an important role of the four mutations that discriminate Dreiklang from Citrine is to shift the p$K_a$ of the on-state chromophore.

Excitation with 500 nm light results in fluorescence with an emission maximum at 529 nm (**Fig. 1b**). Irradiation at the absorption band of the neutral state with light of 405 nm, switched the protein to a non-fluorescent off-state (**Fig. 1c**,**d**). Upon photoswitching to the off-state, a new and unusual absorption band at 340 nm appeared, whereas the absorption bands corresponding to the on-state disappeared (**Fig. 1e**). Subsequent illumination at the 340-nm absorption band of the off-state switched the protein back into the on-state (**Fig. 1c**,**d**). Switching Dreiklang on at 365 nm and off at 405 nm was reversible (**Fig. 1d**). As expected from the p$K_a$ of the on-state chromophore, the fluorescence of Dreiklang could be reversibly switched with a good contrast in a pH range from 6 to 9 (**Supplementary Fig. 1**).

Effective switching could be performed at all physiological temperatures applied (10–40 °C) and was accelerated with increasing temperatures, although the maximal fluorescence was concomitantly reduced at higher temperatures (**Supplementary Fig. 3**). Likewise, the thermal relaxation from the optically induced nonfluorescent state into the equilibrium on-state depends on temperature (**Fig. 1f**, inset). Thermal equilibration was not affected by irradiation at 515 nm (0.82 W/cm$^2$), thus, exciting fluorescence, affected neither the nonfluorescent nor the fluorescent state (**Fig. 1f**), although noticeable cross-talk to the absorption band of the neutral state is anticipated at higher intensities. In living *E. coli* cells expressing Dreiklang, we recorded ~160 switching cycles before the fluorescence was reduced to 50% (at 1.4 W/cm$^2$, 365 nm; 110 W/cm$^2$, 405 nm; 0.82 W/cm$^2$, 515 nm) (**Supplementary Fig. 4**), demonstrating its high switching endurance.

The on-off contrast of the fluorescence signal depends on the sample and the light intensities applied. In widefield images of living mammalian cells, the off-state background signal was <1.4% of the on-state signal (see below), whereas in thick layers of *E. coli* cells, which were used for screening, it was generally 5–10% (**Fig. 1d** and **Supplementary Fig. 4**). In the latter case, we attribute the background mainly to scattering, rather than to ineffective switching.

On native gels, Dreiklang behaves as a monomer (**Supplementary Fig. 5**). Its maturation half-time is ~1.2 h at 30 °C and ~2 h at 37 °C (**Supplementary Fig. 6**). At pH = 7.5, Dreiklang is more resistant to photobleaching than its parent Citrine when using the same light intensities for exciting fluorescence, which may be partly due to Dreiklang's lower extinction coefficient (**Supplementary Fig. 7**).

**Table 1 Properties of Citrine and Dreiklang**

| | Absorbance (nm) | Emission (nm) | QY | ε-max ($M^{-1}cm^{-1}$) | Equilibrium |
|---|---|---|---|---|---|
| Citrine | 515 | 533 | 0.54 | 132,000 | On |
| Dreiklang | $340^{off}/412^{on}/511^{on}$ | 529 | 0.41 | 83,000 | On |

Quantum yield (QY) and extinction coefficient (ε) were measured for the fluorescent on-state protein at pH 7.5.

## Light-driven switching of Dreiklang

To determine the molecular basis for the reversible switching of Dreiklang, we solved the structures of the light-induced off-state (1.7 Å) and on-state (2.0 Å) using the same protein crystal. To this end, a Dreiklang protein crystal in a buffer of pH 4.6 was switched at room temperature (295 K) from the fluorescent equilibrium state into the off-state by irradiation at 405 nm until fluorescence reached a minimum.

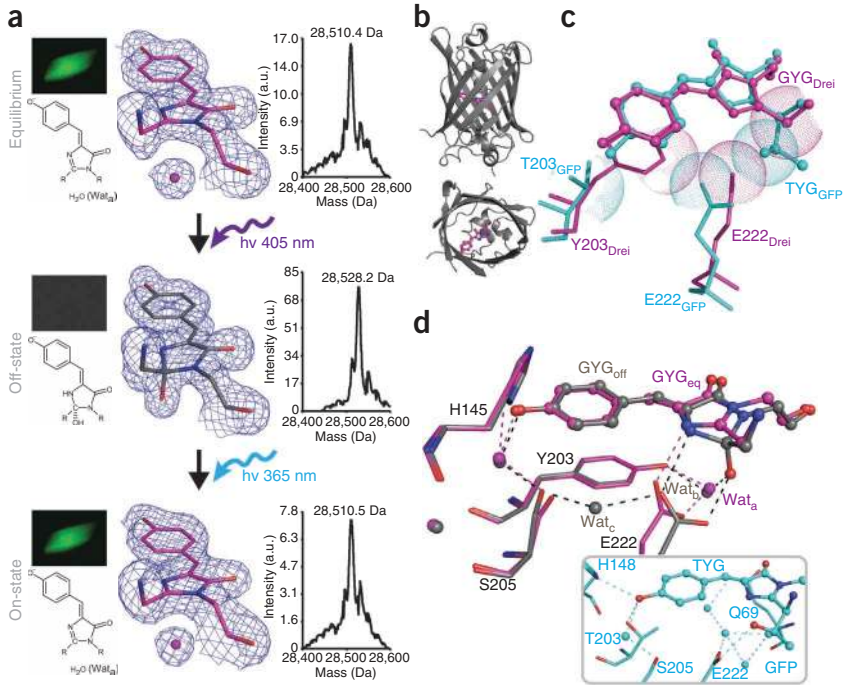


**Figure 2** Molecular basis of Dreiklang photoswitching. (**a**) Dreiklang in the fluorescent equilibrium-state (top), the nonfluorescent off-state (middle) and the fluorescent on-state (bottom). Left, top: representative Dreiklang protein crystal. Left, bottom: proposed chemical structure of the chromophore. Central: details of the X-ray structures (PDB IDs: 3ST2, 3ST3, 3ST4, respectively, top to bottom). Shown is the chromophore (carbon, magenta/gray; oxygen, red; nitrogen, blue). In the equilibrium-state and the on-state, water $Wat_a$ (magenta sphere) is additionally displayed. Final $2F_o–F_c$ electron densities are contoured at the 1σ level. The off-state and the on-state structures have been successively recorded on the same protein crystal. Right: representative deconvoluted ESI-MS spectra of Dreiklang photoswitched in solution and measured under native conditions. (**b**) Overall Dreiklang ribbon structure displayed in two orthogonal views. (**c**) Chromophore and immediate surrounding of on-state Dreiklang (magenta) and GFP (PDB: 1EMA[25]) (cyan). The Van-der-Waals' radii of important atoms are indicated by spheres to highlight structural restraints. The chromophores are depicted as ball and stick whereas the surrounding amino acid residues are shown in the stick representation. (**d**) Superimposed representations of the Dreiklang hydrogen bond network in the (fluorescent) equilibrium- and the off-states. Equilibrium-state carbons, magenta; off-state carbons, gray; oxygen, red; nitrogen, blue. Important water molecules are shown as magenta (equilibrium-state) and gray (off-state) spheres. Inset: hydrogen bond network in GFP.



After the off-state diffraction data was recorded at 100 K, we warmed the very same crystal of Dreiklang back to 295 K, switched it by irradiation with 365 nm light until the fluorescence reached a maximum and recorded the on-state diffraction data at 100 K. In addition, we solved the X-ray structure of Dreiklang in the fluorescent equilibrium-state to a resolution of 1.9 Å (**Fig. 2**). Notably, the kinetics of the thermal equilibration of the fluorescence signal after switching off was comparable for Dreiklang in solution and in the crystal (**Supplementary Fig. 8**), indicating that the crystal lattice did not have major effects on the switching behavior.

The overall structure of Dreiklang resembles that of GFP and related proteins (**Fig. 2b**). The chromophore, autocatalytically formed from the Gly65-Tyr66-Gly67 tripeptide, resides in an alpha-helical segment, enclosed by an 11-stranded beta-barrel. As expected from the similar spectroscopic properties, the on-state structure was practically superimposable on the fluorescent equilibrium-state structure. The on-state chromophore consists of an imidazolinone-ring, connected by a methine bridge to a *p*-hydroxyphenyl ring. The two rings of the chromophoric systems were largely co-planar, facilitating a conjugated pi-electron system and hence supporting fluorescence.

In the off-state, the *p*-hydroxyphenyl ring lies largely in plane with the $C_{\alpha 66}$-$C_{\beta 66}$ bond, as well as with the $C_{\alpha 66}$-$C_{66}$ and the $C_{\alpha 66}$-$N_{66}$ bonds, indicating that the methine bridge connecting the two rings is maintained. However, in the off-state structure, the planarity of the five-membered ring was markedly distorted with the chromophoric $C_{65}$ exhibiting a tetrahedral geometry indicative of an $sp^3$ hybridization. A clear signal in the electron density map indicates a new hydroxyl group at the $C_{65}$ atom, suggesting that the imidazolinone ring was converted into a 2-hydroxyimidazolidinone ring (**Fig. 2a** and **Supplementary Fig. 9**). We propose that the hydration of the imidazolinone ring shortens the chromophoric pi-electron system, resulting in the new absorption band at 340 nm and the simultaneous disappearance of the absorption bands at 412 and 511 nm (**Fig. 1e**).

To further confirm this light-induced chemical modification, we carried out electrospray ionization mass spectrometry (ESI-MS). To this end, switching of Dreiklang in solution (pH 6.9; 295 K) was monitored by measuring the fluorescence signal; the proteins in the respective states were immediately analyzed by ESI-MS under native conditions (in 18% acetonitrile). We found a mass difference of 18 ± 0.3 Da between the nonfluorescent state and the light-induced on-state or the equilibrium state, respectively (**Fig. 2a** and **Supplementary Figs. 10** and **11**). This strongly indicates the reversible covalent addition of a water molecule that occurred parallel to changes in the fluorescence signal. Hence, the ESI-MS data are in full agreement with the X-ray data, supporting the view of a reversible light-induced covalent chemical modification, that is, a hydration-dehydration reaction of the chromophoric five-membered ring as the underlying molecular mechanism of switching in Dreiklang.

A similar reversible hydration reaction was postulated, although controversially discussed, to occur during the chromophore formation of GFP[27–29]. This might suggest that the light-induced reversible switching of Dreiklang is based on a molecular reaction that is possibly occurring during chromophore maturation of some fluorescent proteins. Hence, we propose that Dreiklang may be used as a scaffold for further engineering and that this switching mechanism may be transferred to other fluorescent proteins.

Our mutagenesis studies showed that the amino acid residues Y203 and E222 as well as the chromophore building G65 are crucial for the unusual switching characteristics of Dreiklang. The amino acids G65 and Y203 facilitate the positioning of the side chain of E222 close to the imidazolinone ring (**Fig. 2c**). In the fluorescent-state, Y203 and E222 form hydrogen bonds to a water molecule ($Wat_a$) and thereby stabilize it in close vicinity to the $C_{65}$ of the chromophore (**Fig. 2d**), a situation that is different in the nonswitchable GFP (avGFP-S65T)[25] (**Fig. 2d**, inset). In GFP, a water molecule corresponding to $Wat_a$ is stabilized by water-mediated H-bonds only. We propose that $Wat_a$ is

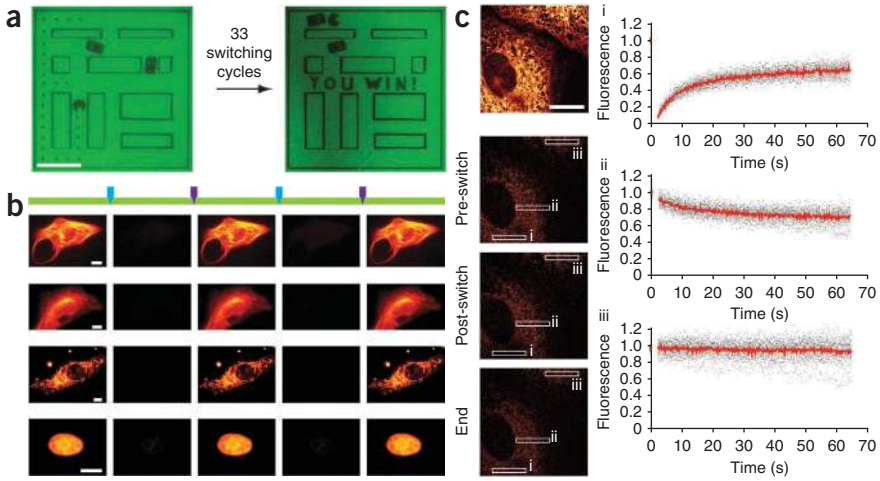


**Figure 3** Applications of Dreiklang. (**a**) 'PacMan' movie. Thirty-three individual images were written successively at the same position of a polyacrylamide-Dreiklang layer. Before writing each new frame, all molecules were photoswitched to the on-state. Shown are the first and the thirty-third frame (see also **Supplementary Movie 1**). Scale bar, 100 µm. (**b**) Switching of various Dreiklang fusion proteins in living Vero cells (from left to right, on, off, etc.). From top to bottom: Dreiklang-MAP2, Dreiklang-α-tubulin, mito-Dreiklang, Dreiklang-Histone2B. Fluorescence was excited with green light (495 nm); switch-off (light blue arrowheads): near-UV (420 nm); switch-on (violet arrowheads): UV-light (360 nm). (**c**) FRAS with Dreiklang. Dreiklang was targeted to the ER in living Vero cells. Images from top to bottom: overview; before switching; immediately after switching Dreiklang off in region of interest (ROI)-i; and at the end of the measurement (65 s after switching). Graphs on the right: the plotted fluorescence signals were collected within the indicated ROIs during 20 repetitions of the same FRAS experiment on a single cell (ROI-i: in this region Dreiklang was selectively switched off prior to the measurement; ROI-ii: in the same cell, showing the flow of switched-off Dreiklang molecules into this region; ROI-iii: in the neighboring cell). Shown are raw data. The red line marks the mean values at each time point, demonstrating the reduction of statistical noise. Scale bars in **b** and **c**, 10 µm.



important for the light-driven off-switching in Dreiklang, because it appears to be in a suitable position for a nucleophilic addition across the C=N bond of the imidazolinone ring.

The off-state structure reveals a new water molecule ($Wat_b$) displaced by 1.02 ± 0.09 Å from the position of $Wat_a$. It is held in this position by a differently configured hydrogen bonding network. We found during occupancy refinement of $Wat_b$ that the occupancy was significantly smaller than 1.0 (e.g., chain C: 0.35), strongly indicating that this position is not always occupied by a water molecule in the off-state protein. Hence we assume that $Wat_b$ is taken up from the environment after $Wat_a$ has been used for the light-induced hydration of the imidazolinone ring upon switching from the on- to the off-state.

Altogether, these findings lend support to a reversible light-induced hydration/dehydration reaction of the five-membered ring. In the on-state, the chromophore exists in the protonated and the deprotonated form, resulting in absorption bands at 412 nm and 511 nm, respectively. Irradiation at the 511-nm band induces fluorescence, whereas irradiation at the 412-nm band induces a covalent modification (hydration) of the five-membered ring, resulting in a nonfluorescent chromophore absorbing at 340 nm. Subsequent irradiation at this band results in a dehydration of the off-state chromophore converting it back into the on-state chromophore. Although the reversible water addition/elimination reaction appears to be the key factor in the unusual switching behavior of Dreiklang, it is possible that additional short-lived intramolecular rearrangements may occur, possibly including a *cis-trans* isomerization, structural flexibility or a strong bending of the chromophore.

### Use of Dreiklang for fluorescence recovery after switching

To evaluate the properties of Dreiklang for imaging purposes, we prepared a layer of purified Dreiklang molecules and wrote complex patterns[6,30,31] into this layer showing that Dreiklang can be exploited for reversibly recording and reading information (**Fig. 3a** and **Supplementary Movie 1**). Next, we generated several fusion proteins, namely Dreiklang-Map2, Dreiklang-α-tubulin, Dreiklang-histone2B, keratin19-Dreiklang, vimentin-Dreiklang, β-actin-Dreiklang and Dreiklang targeted to the mitochondrial matrix (Mito-Dreiklang) and expressed these fusion proteins in cultivated mammalian cells (**Fig. 3b** and **Supplementary Fig. 12**). The fact that Dreiklang could be functionally fused to α-tubulin and histone2B demonstrates that Dreiklang behaves as a monomer also *in vivo*. Targeted to the different cellular structures, Dreiklang could be switched on and off in living cells repeatedly (**Fig. 3b**).

Because switching Dreiklang on and off requires UV and near-UV light, we were concerned that this irradiation might negatively affect the viability of the cells. To investigate this issue, we expressed vimentin-Dreiklang in PtK2 cells. The Dreiklang fluorescence was switched 100 times on and off in whole living cells with widefield illumination, displaying a contrast in the fluorescence signal of around 75:1 in each cycle (**Supplementary Fig. 13** and **Supplementary Movie 2**). No major alterations in the labeled structures were observed during this period (~10 min). Next, we targeted Dreiklang to the endoplasmic reticulum (ER) of PtK2 cells and switched the ability to fluoresce 5 or 20 times on and off (**Supplementary Fig. 14**). We found that five switching cycles had no detectable effect on the viability of the cells after 2 h compared to the control where switching was omitted. After 20 cycles, ~16% of the cells were dead after 2 h ($n$ = 300 cells, six independent experiments) and a larger and highly variable fraction of cells showed changes in their shapes. This finding demonstrates that repeated irradiation with UV light is unfavorable but does not necessarily induce cell death. However, most practical applications will require either fewer switching cycles and/or much smaller regions exposed to UV light for switching, which thus would reduce the overall light dose by at least an order of magnitude and the effects on the cellular viability accordingly.

As a demonstration that Dreiklang's properties can be exploited for repeated measurements of protein dynamics in individual living cells, we expressed Dreiklang targeted to the ER in Vero cells (**Fig. 3c**). Using a commercial confocal microscope, we selectively photoswitched (with 405 nm) ER-Dreiklang in one region of the living cell from the fluorescent into the nonfluorescent state and followed the movement of nonswitched on-state molecules into the switched-off region by probing fluorescence with 515 nm. After the measurement, the fluorophores in the whole cell were switched back to the initial fluorescent state with 360 nm using wide-field illumination; the

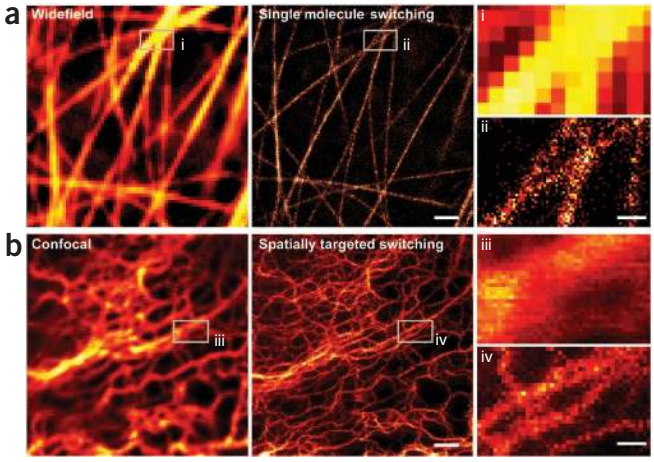


**Figure 4** Super-resolution microscopy of living PtK2 cells using Dreiklang. (**a**) Cells expressing Dreiklang-Map2 imaged both conventionally (left) and by super-resolution microscopy based on single-molecule stochastic switching (center). (**b**) Keratin19-Dreiklang expressed in living cells and imaged both confocally (left) and in the RESOLFT mode (spatially targeted switching) (center). Right: magnifications of the regions indicated in the main images. Scale bars, 1 µm (middle, left), 250 nm (right).

measurement, which was substantially shorter (65 s) than the thermal equilibration of Dreiklang to the on-state, was repeated several tens of times. We denominate this approach as fluorescence recovery after switching (FRAS). Individual measurements of cellular protein movements often exhibit statistical noise[32–34], which was strongly reduced in FRAS by averaging over many switching cycles. Analogous approaches have previously been done using conventional RSFPs or photoactivatable proteins[16,35].

### Nanoscopy with Dreiklang

To overcome the diffraction barrier, all super-resolution (nanoscopy) concepts use a molecular mechanism to sequentially inhibit the fluorescence of adjacent features[36]. Two families of approaches rest on this principle. In the first family, which has been termed RESOLFT (reversible saturable optical (fluorescence) transitions between two states), the sample coordinates at which the fluorophores are on and off are predefined by a pattern of light[6,8,36]. In the second family encompassing (F)PALM, STORM and others[9,10,36,37], individual fluorophores are switched on and off stochastically, whereby the coordinate of the emitting molecule is found using the photons detected on a camera. We reasoned that the decoupling of fluorescence switching from excitation in Dreiklang would enable additional possibilities for super-resolution microscopy.

In the stochastic methods, the number of emitted photons and the emission rate of a molecule in the on-state together determine the localization precision and the recording time. Although these parameters are difficult to control in conventional fluorescent proteins or RSFPs, in Dreiklang the on-time can be influenced by adapting the light intensities used for switching on and off, eventually even interactively in response to the local fluorophore densities. We fused Dreiklang to Map2 and expressed the fusion construct in PtK2 cells. The cells were initially irradiated for 10 s at 405 nm (0.2 kW/cm$^2$) to switch the majority of Dreiklang proteins off. Subsequently we recorded 8,000 image frames (10 ms each) with irradiation at 491 nm (2 kW/cm$^2$). Between two frames the cells were irradiated for 0.1–0.5 µs with light of 405 nm and/or 355 nm (2 W/cm$^2$) to adjust the number of on-state fluorophores to less than one per diffraction area. We obtained an average localization precision of ~15 nm using ~700 detected photons, resulting in images that were clearly superior to the conventional counterparts (**Fig. 4a**).

We also realized an implementation based on spatially targeted switching of the fluorophores (RESOLFT)[6,8]. We imaged living PtK2 cells expressing keratin19-Dreiklang by first switching Dreiklang on at 355 nm (1 ms, 160 W/cm$^2$) using a regular shaped, diffraction-limited focus. Then, a doughnut-shaped focus of light of 405 nm (40 ms, 110 W/cm$^2$) with a central intensity minimum (zero) was used for switching Dreiklang off at the focal periphery only. Finally, fluorescence was probed by 491 nm excitation (4 kW/cm$^2$) for 10 ms. The image was generated by scanning over the sample using this irradiation scheme at every pixel (**Fig. 4b**). The Dreiklang images taken in the RESOLFT mode reveal many details with a resolution of down to ~35 nm (**Supplementary Fig. 15**) that are fully blurred in the corresponding confocal data. Note that the presented image data are raw.

## DISCUSSION

The photoswitching of Dreiklang is based on a light-driven reversible hydration-dehydration reaction modifying the chromophore, which uniquely decouples the switching spectra from their excitation counterpart. Thus Dreiklang allows fine-tuning of the duration of the chromophore states without interference by the fluorescence excitation light.

This feature provides benefits for super-resolution microscopy techniques applying stochastic single-molecule switching (**Fig. 4a**) and spatially targeted switching (**Fig. 4b**), but should also enable applications that would be difficult or even impossible with conventional switchable fluorescent proteins. Among others, this includes FRAS (**Fig. 3c**), allowing multiple bleaching or photoactivation measurements in single cells, potentially enabling a new generation of single cell–based screening approaches. One may also envision sophisticated Förster resonance energy transfer (FRET) measurements with multiple fluorophores using Dreiklang as an additional switchable component. Dreiklang may also provide new avenues to multicolor applications in combination with other RSFPs or conventional fluorescent proteins. In this case, contrast may be obtained either by switching[19], or by different colors or by dissimilar fluorescence lifetimes. In addition to applications in life sciences, the decoupling of switching from fluorescence excitation should also offer new options in subdiffraction reading and writing in protein layers.

Long-term protein tracking will require Dreiklang variants with longer lifetimes of the metastable states. Likewise, it is conceivable to design proteins offering even more switching cycles and operating with longer wavelengths. With its X-ray structure available, we anticipate the specific generation of further Dreiklang derivatives forming a new class of switchable fluorescent proteins.

## METHODS

Methods and any associated references are available in the online version of the paper at http://www.nature.com/naturebiotechnology/.

**Accession code.** The atomic coordinates and structure factors have been deposited in the Protein Data Bank, http://www.pdb.org (PDB ID codes 3ST2, 3ST3 and 3ST4).

*Note: Supplementary information is available on the Nature Biotechnology website.*

ACKNOWLEDGMENTS

We acknowledge access to beamline BL14.2 of the BESSY II storage ring (Berlin) through the Joint Berlin MX-Laboratory sponsored by the Helmholtz Zentrum Berlin für Materialien und Energie, the Freie Universität Berlin, the Humboldt-Universität zu Berlin, the Max-Delbrück Centrum and the Leibniz-Institut für

Molekulare Pharmakologie. We thank V. Belov for insightful discussions and F. Lavoie-Cardinal for help with the set-up for targeted switching. We acknowledge A. Schönle for providing the software ImSpector. We also thank T. Gilat, S. Löbermann, R. Pick and E. Rothermel for excellent technical assistance, H.-H. Hsiao for help in ESI-MS and H. Schill and J. Jethwa for carefully reading the manuscript. We acknowledge R.Y. Tsien for sharing the plasmid pRSET-Citrine. This work was supported by the Deutsche Forschungsgemeinschaft through the Gottfried Wilhelm Leibniz Prize (to S.W.H.) and through the DFG-Research Center for Molecular Physiology of the Brain (to S.J.).

## AUTHOR CONTRIBUTIONS

G.W., M.A. and I.T. contributed equally to this work. C.E., S.W.H. and S.J. conceived the project. T.B., A.C.S., G.W., M.A., I.T., T.G., M.L. and U.P. performed all experiments. I.T. recorded the super-resolution images. Data analysis was done by T.B., A.C.S., G.W., M.A., I.T., T.G., M.L., H.U., C.E., M.C.W., S.W.H. and S.J. The manuscript was written by S.W.H. and S.J. All authors discussed the results and commented on the manuscript.

## COMPETING FINANCIAL INTERESTS

The authors declare competing financial interests: details accompany the full-text HTML version of the paper at http://www.nature.com/nbt/index.html.

Published online at http://www.nature.com/nbt/index.html.
Reprints and permissions information is available online at http://www.nature.com/reprints/index.html.



1. Tsien, R.Y. The green fluorescent protein. *Annu. Rev. Biochem.* **67**, 509–544 (1998).
2. Lippincott-Schwartz, J., Altan-Bonnet, N. & Patterson, G.H. Photobleaching and photoactivation: following protein dynamics in living cells. *Nat. Cell Biol.* S7–S14 (2003).
3. Lukyanov, K.A., Chudakov, D.M., Lukyanov, S. & Verkhusha, V.V. Innovation: photoactivatable fluorescent proteins. *Nat. Rev. Mol. Cell Biol.* **6**, 885–890 (2005).
4. Dickson, R.M., Cubitt, A.B., Tsien, R.Y. & Moerner, W.E. On/off blinking and switching behaviour of single molecules of green fluorescent protein. *Nature* **388**, 355–358 (1997).
5. Habuchi, S. *et al.* Reversible single-molecule photoswitching in the GFP-like fluorescent protein Dronpa. *Proc. Natl. Acad. Sci. USA* **102**, 9511–9516 (2005).
6. Hell, S.W., Jakobs, S. & Kastrup, L. Imaging and writing at the nanoscale with focused visible light through saturable optical transitions. *Appl. Phys. A Mater. Sci. Process.* **77**, 859–860 (2003).
7. Hell, S.W. Toward fluorescence nanoscopy. *Nat. Biotechnol.* **21**, 1347–1355 (2003).
8. Hofmann, M., Eggeling, C., Jakobs, S. & Hell, S.W. Breaking the diffraction barrier in fluorescence microscopy at low light intensities by using reversibly photoswitchable proteins. *Proc. Natl. Acad. Sci. USA* **102**, 17565–17569 (2005).
9. Betzig, E. *et al.* Imaging intracellular fluorescent proteins at nanometer resolution. *Science* **313**, 1642–1645 (2006).
10. Hess, S.T., Girirajan, T.P. & Mason, M.D. Ultra-high resolution imaging by fluorescence photoactivation localization microscopy. *Biophys. J.* **91**, 4258–4272 (2006).
11. Patterson, G.H. & Lippincott-Schwartz, J. A photoactivatable GFP for selective photolabeling of proteins and cells. *Science* **297**, 1873–1877 (2002).
12. Chudakov, D.M. *et al.* Photoswitchable cyan fluorescent protein for protein tracking. *Nat. Biotechnol.* **22**, 1435–1439 (2004).
13. Subach, F.V. *et al.* Photoactivatable mCherry for high-resolution two-color fluorescence microscopy. *Nat. Methods* **6**, 153–159 (2009).
14. Lukyanov, K.A. *et al.* Natural animal coloration can be determined by a nonfluorescent green fluorescent protein homolog. *J. Biol. Chem.* **275**, 25879–25882 (2000).
15. Cinelli, R.A.G. *et al.* Green fluorescent proteins as optically controllable elements in bioelectronics. *Appl. Phys. Lett.* **79**, 3353–3355 (2001).
16. Ando, R., Mizuno, H. & Miyawaki, A. Regulated fast nucleocytoplasmic shuttling observed by reversible protein highlighting. *Science* **306**, 1370–1373 (2004).
17. Henderson, J.N., Ai, H.W., Campbell, R.E. & Remington, S.J. Structural basis for reversible photobleaching of a green fluorescent protein homologue. *Proc. Natl. Acad. Sci. USA* **104**, 6672–6677 (2007).
18. Stiel, A.C. *et al.* 1.8 Å bright-state structure of the reversibly switchable fluorescent protein Dronpa guides the generation of fast switching variants. *Biochem. J.* **402**, 35–42 (2007).
19. Andresen, M. *et al.* Photoswitchable fluorescent proteins enable monochromatic multilabel imaging and dual color fluorescence nanoscopy. *Nat. Biotechnol.* **26**, 1035–1040 (2008).
20. Stiel, A.C. *et al.* Generation of monomeric reversibly switchable red fluorescent proteins for far-field fluorescence nanoscopy. *Biophys. J.* **95**, 2989–2997 (2008).
21. Adam, V. *et al.* Structural characterization of IrisFP, an optical highlighter undergoing multiple photo-induced transformations. *Proc. Natl. Acad. Sci. USA* **105**, 18343–18348 (2008).
22. Subach, F.V. *et al.* Red fluorescent protein with reversibly photoswitchable absorbance for photochromic FRET. *Chem. Biol.* **17**, 745–755 (2010).
23. Sinnecker, D., Voigt, P., Hellwig, N. & Schaefer, M. Reversible photobleaching of enhanced green fluorescent proteins. *Biochemistry* **44**, 7085–7094 (2005).
24. Shaner, N.C. *et al.* Improving the photostability of bright monomeric orange and red fluorescent proteins. *Nat. Methods* **5**, 545–551 (2008).
25. Ormö, M. *et al.* Crystal structure of the *Aequorea victoria* green fluorescent protein. *Science* **273**, 1392–1395 (1996).
26. Griesbeck, O., Baird, G.S., Campbell, R.E., Zacharias, D.A. & Tsien, R.Y. Reducing the environmental sensitivity of yellow fluorescent protein – Mechanism and applications. *J. Biol. Chem.* **276**, 29188–29194 (2001).
27. Siegbahn, P.E.M., Wirstam, M. & Zimmer, M. Theoretical study of the mechanism of peptide ring formation in green fluorescent protein. *Int. J. Quantum Chem.* **81**, 169–186 (2001).
28. Rosenow, M.A., Huffman, H.A., Phail, M.E. & Wachter, R.M. The crystal structure of the Y66L variant of green fluorescent protein supports a cyclization-oxidation-dehydration mechanism for chromophore maturation. *Biochemistry* **43**, 4464–4472 (2004).
29. Barondeau, D.P., Kassmann, C.J., Tainer, J.A. & Getzoff, E.D. Understanding GFP chromophore biosynthesis: controlling backbone cyclization and modifying post-translational chemistry. *Biochemistry* **44**, 1960–1970 (2005).
30. Irie, M., Fukaminato, T., Sasaki, T., Tamai, N. & Kawai, T. Organic chemistry: a digital fluorescent molecular photoswitch. *Nature* **420**, 759–760 (2002).
31. Sauer, M. Reversible molecular photoswitches: a key technology for nanoscience and fluorescence imaging. *Proc. Natl. Acad. Sci. USA* **102**, 9433–9434 (2005).
32. Lippincott-Schwartz, J., Snapp, E. & Kenworthy, A. Studying protein dynamics in living cells. *Nat. Rev. Mol. Cell Biol.* **2**, 444–456 (2001).
33. Phair, R.D. & Misteli, T. Kinetic modelling approaches to *in vivo* imaging. *Nat. Rev. Mol. Cell Biol.* **2**, 898–907 (2001).
34. Sprague, B.L. & McNally, J.G. FRAP analysis of binding: proper and fitting. *Trends Cell Biol.* **15**, 84–91 (2005).
35. Chudakov, D.M., Chepurnykh, T.V., Belousov, V.V., Lukyanov, S. & Lukyanov, K.A. Fast and precise protein tracking using repeated reversible photoactivation. *Traffic* **7**, 1304–1310 (2006).
36. Hell, S.W. Microscopy and its focal switch. *Nat. Methods* **6**, 24–32 (2009).
37. Rust, M., Bates, M. & Zhuang, X. Sub-diffraction-limit imaging by stochastic optical reconstruction microscopy (STORM). *Nat. Methods* **3**, 793–796 (2006).

## ONLINE METHODS

**Cloning.** *Constructs for bacterial expression.* For protein expression and mutagenesis, the respective coding sequences were PCR amplified, digested and inserted into the BamHI/HindIII restriction sites of the plasmid pQE31 (Qiagen).

*Constructs for expression in mammalian cells.* To target Dreiklang to the lumen of the endoplasmic reticulum (ER), the coding sequence of Dreiklang was amplified by PCR using the primers 5′-CTGCAGGTCGACATGGTGAGCAAGGGCGAGGA-3′ and 5′-TTCTGCGGCCGCCTTGTACAGCTCGTCCATGCCGCCGGT-3′. The PCR fragments were digested with SalI and NotI and inserted into the vector pEF/myc/ER (Invitrogen).

To target Dreiklang to the mitochondrial matrix, the coding sequence of Dreiklang was amplified by PCR using the primers 5′-TCCACCGGTCGCCACCATGGTGAGCAAGGGCGAGGAGCTGTTC-3′ and 5′-GTCGCGGCCGCTACTTGTACAGCTCGTCCATGCCGAGAG-3′. The PCR fragments were digested with AgeI and NotI and inserted into the vector pDsRed1-Mito (Clontech), replacing the DsRed1 sequence.

For the generation of the α-tubulin fusion construct, the Dreiklang coding sequence was amplified by PCR using the primers 5′-GATCCGCTAGCGCTAATGGTGAGCAAGGGCGAGGAG-3′ and 5′-CACTCGAGATCTGAGTCCGGACTTGTACAGCTCGTCCATGCC-3′. The PCR fragments were digested with NheI and BglII and inserted into the vector pEGFP-Tub (Clontech), replacing the EGFP sequence.

For the generation of the microtubule-associated protein 2 (Map2) fusion construct, the Map2 coding sequence (obtained from pDONR223-MAP2) was amplified by PCR using the primers 5′-GATCTCGAGTGATGGCAGATGAACGGAAAGACGAAGC-3′ and 5′-GGTGGATCCTTATCACAAGCCCTGCTTAGCGAGTGCAGC-3′. The PCR fragments were digested with XhoI and BamHI and inserted into the vector Dreiklang-α-tubulin, replacing the α-tubulin sequence.

For the generation of the Histon-2B fusion construct, the Histon-2B coding sequence (obtained from pDONR223-HIST1H2BN[38]) was amplified by PCR using the primers 5′-GATCTCGAGTGATGCCCGAGCCCTCAAAGTCCGCTCCTGCCCC-3′ and 5′-GGTGGATCCTTATCAATCTCTTGCAATATAAATGTCATCTGG-3′. The PCR fragments were digested with XhoI and BamHI and inserted into the vector Dreiklang-α-tubulin, replacing the α-tubulin sequence.

To create fusion constructs of Dreiklang with vimentin, keratin19 and beta-actin, Dreiklang was amplified using the primers 5′-GATCCACCGGTCGCGGCGTGAGCAAGGGCGAGGAGCTG-3′ and 5′-ACAACTTAAGAACAACAATTGTTACTTGTACAGCTCGTCCATGCC-3′. The PCR fragment was cloned into the gateway destination vector pMD-tdEosFP-N[39] using the restriction sites AgeI and AflII, thereby replacing the tdEosFP coding sequence against the Dreiklang sequence. The final plasmids pMD-Vim-Dreiklang, pMD-Ker19-Dreiklang and pMD-ACTB-Dreiklang were constructed by gateway vector conversion (Invitrogen) using the donor vectors pDONR223-Vim, pDONR223-Krt19 and pDONR223-ACTB[38].

**Mutagenesis.** For site-directed random mutagenesis, the QuikChange Site-Directed Mutagenesis Kit (Stratagene) was used according to the manufacturer's instructions. Error-prone random mutagenesis and directed simultaneous mutagenesis of multiple sites were performed according to standard protocols.

**Protein expression and purification.** Proteins were expressed in the *Escherichia coli* strain BL21-CodonPlus (Stratagene) and purified by Ni-NTA affinity chromatography, followed by a gel-filtration step on a Superdex 200 column (Amersham Biosciences) using a Tris-buffer (100 mM Tris-HCl, 150 mM NaCl, pH 7.5).

**Protein characterization.** *Semi-native PAGE.* Proteins (10 µg each) were loaded onto 15% polyacrylamide gels containing 0.1% sodiumdodecyl sulfate (SDS). For loading, proteins were taken up in a 60% (wt/vol) sucrose solution. As size standards, purified monomeric EGFP and Citrine, dimeric dTomato and tetrameric DsRed were used.

*Protein and chromophore maturation.* An overnight TOP10 *E. coli* culture (Invitrogen) transformed with the pBad-Dreiklang plasmid, grown at 37 °C in LB medium supplemented with ampicillin was used to inoculate 200 ml of $LB_{Amp}$ medium. After the bacterial cells were grown at 37 °C to an $OD_{600}$ of 0.5, protein expression was induced by adding arabinose to a final concentration of 0.2%. After 4 h of further incubation at 37 °C, cells were pelleted and disrupted. Dreiklang proteins were immediately purified using His SpinTrap columns (GE Healthcare) within 20 min and kept strictly at 4 °C. The purified protein solution was diluted in buffer (final buffer concentration: 20 mM sodium phosphate, 500 mM NaCl, 30 mM imidazole pH 7.5) and then filled into QS cuvettes, which were incubated at 30 °C and 37 °C, respectively. For assessment of maturation, fluorescence emission spectra were taken with a Varian Cary Eclipse fluorescence spectrometer (Varian), at the indicated time points.

*Absorption and emission spectra.* Absorption and emission spectra were recorded on a Varian Cary 4000 UV/VIS spectrophotometer and a Varian Cary Eclipse fluorescence spectrometer (Varian), respectively. Quantum yields and extinction coefficients were determined in comparison to EGFP[40]. The indicated values are the means of three independent protein purifications.

*Photoswitching.* Switching of Dreiklang or Citrine fluorescence was recorded either on *E. coli* colonies grown on LB-agar plates (**Fig. 1c**,**d** and **Supplementary Fig. 4**) or in various buffered protein solutions. For recording of the switching at various temperatures purified Dreiklang was taken up in 100 mM Tris-HCl, 150 mM NaCl, pH 7.5. A modified computer-controlled fluorescence microscope (Leica Microsystems) equipped with a 50× NA 0.5 or a 20× NA 0.4 air objective lens and three 100 W Hg lamps was used for data acquisition. Different excitation filters (365/25, 405/10, 595/10, LOT Oriel) and shutters (Melles Griot) in front of each lamp facilitated the controlled on- and off-switching and the fluorescence recording. Fluorescence was recorded using a photomultiplier tube (HR9306-0, Hamamatsu) behind a 525 nm longpass detection filter (HQ 525 LP, AHF Analysentechnik).

*Relaxation half-times.* For the determination of the relaxation half-time from the nonfluorescent off-state into the fluorescent on-state (thermal equilibrium), purified Dreiklang (at pH 7.5) was switched completely into the off-state and the relaxation to the equilibrium state was followed by consecutive short pulses or continuous irradiation with light of 515 nm. For details on the used intensities and the timing see **Supplementary Table 1**. These experiments were performed at the indicated temperatures in a temperature-controlled environment.

The thermal relaxation of Dreiklang from the light-driven off-state into the equilibrium state in living cells was determined on PtK2 cells expressing Dreiklang in the ER using a wide-field epifluorescence microscope. For the measurements, Dreiklang was first switched into the nonfluorescent state (4 s, 405/10 nm, 80 W/cm$^2$). Subsequently, images were recorded (515/10 nm, 2.6 W/cm$^2$) at different time points to monitor the thermal relaxation. Finally, the cells were irradiated with light of 365/25 nm (5 s, 3.4 W/cm$^2$) and an image providing the maximal fluorescence was recorded. For analysis, regions of interest were selected within the cells. For background subtraction the fluorescence signal next to the respective cells was used.

**Imaging.** For imaging of mammalian cells, Vero cells (kidney epithel cells of *Cercopithecus aethiops*) or PtK2 cells (kidney epithel cells of *Potorous tridactylis*) were transfected with the respective plasmids by the Nanofectin Kit (PAA) according to the manufacturer's instructions. The cells were propagated in DMEM medium with GlutaMAX and 4.5 g/l glucose, 10% (vol/vol) FCS, 1 mM sodium pyruvate, 50 mg/ml penicillin and 50 mg/ml streptomycin. Cells were grown on coverslips in Petri dishes at 37 °C (310 K) under 90% humidity and 5% $CO_2$.

*Repeated switching of Dreiklang embedded in polyacrylamide (PAA).* A solution of Dreiklang molecules was embedded in PAA (final concentration: 15% PAA in 1.5 M Tris/HCl buffer, pH 8.8) and squeezed under a coverslip to ensure a layer thickness of ~1 µm. For reading and writing a Leica SP5 beam scanning confocal microscope equipped with a 40× NA 1.25 oil immersion objective





doi:10.1038/nbt.1952

was used. The following settings were used: pinhole, 1.48 AU; pixel size, 378.8 nm × 378.8 nm; scan speed, 400 Hz. Fluorescence was detected between 517 and 575 nm. Except for smoothing and contrast stretching, no further image processing was applied.

To generate the PacMan-movie (**Fig. 3a** and **Supplementary Movie 1**), each individual image was written using a group of ROIs, defining the positions where Dreiklang was transferred from the on- to the off-state by irradiation with 405 nm laser-light (4.3 MW/cm$^2$). Subsequently the written image was recorded with 515 nm laser-irradiation (2.4 kW/cm$^2$) only. In the next step all proteins were switched back to the fluorescent state with 360 nm wide-field illumination (0.1 W/cm$^2$, BP360nm/40nm, 5 s) and the next image was recorded.

*Widefield measurements.* For widefield imaging (**Fig. 3b**) a Leica DM6000 epifluorescence microscope (Leica) equipped with a 100× NA 1.40 oil immersion objective lens and a DFC350 FX camera (Leica) was used. Cells were irradiated for 300 ms with near-UV light (420/30 nm, 15 W/cm$^2$) to switch the Dreiklang molecules to the nonfluorescent state and 300 ms with UV light (360/40 nm, 5 W/cm$^2$) to switch the proteins back to the fluorescent state. The fluorescence images were recorded with green light (495/15 nm, 13 W/cm$^2$). For fluorescence detection, a 510 nm dichroic mirror and a 530/30 nm detection filter were used. The length of the image acquisition time was adjusted to the brightness of every sample and was generally between 50 and 150 ms.

To record 100 switching cycles of Dreiklang in living mammalian cells (**Supplementary Fig. 13** and **Supplementary Movie 2**), the same microscope settings were used. Switching times were 800 ms (near-UV) and 100 ms (UV). Images were recorded with an acquisition time of 100 ms.

*Confocal microscopy.* Confocal imaging (**Supplementary Fig. 12**) was performed with a beam scanning confocal microscope (SP5, Leica Microsystems) equipped with a UV-corrected NA 1.4 oil immersion lens (63× HCX PL APO). All imaging was performed at ~25 °C. For excitation, light of 515 nm was used, fluorescence was detected between 520 and 600 nm.

*FRAS.* Imaging was performed with a beam scanning confocal microscope (SP5, Leica Microsystems) equipped with a UV-corrected NA 1.4 oil immersion lens (63× HCX PL APO). All imaging was performed at ~25 °C. The following microscope settings were used: pinhole, 1 Airy unit (AU); pixel size, 160.8 nm × 160.8 nm; scan speed, 1,400 Hz. Fluorescence was detected between 519 and 590 nm.

For each measurement, the Dreiklang molecules in an ROI (1.3 µm × 10 µm) were switched to the nonfluorescent state using 405 nm laser light (2.7 MW/cm$^2$). The fluorescence was recorded by excitation with 515 nm laser light (1.5 kW/cm$^2$). Finally, the Dreiklang molecules in the whole sample were switched to the fluorescent state with 360 nm (BP360 nm/40 nm; 1 s; 0.6 W/cm$^2$) widefield illumination. This imaging sequence was repeated several times on the same cell. In every sequence a second ROI on the other side of the same cell and a third ROI in a neighboring cell were analyzed. No further data processing was performed, except background subtraction and normalization to 1.

*Analysis of the influence of irradiation on cell viability.* Imaging was performed with an epi-fluorescence microscope equipped with a custom-built incubator chamber to maintain the temperature at 37 °C and a water immersion objective (HCX APO L 20×/0.50 W U-V-I). At the end of the experiment, cells were incubated for 15 min with Sytox AADvanced Dead Cell Stain (Invitrogen). Switching was carried out by irradiation with light of 405/10 nm (24 W/cm$^2$ for 4 s) to switch off and 365/25 nm (1 W/cm$^2$ for 6 s) to switch on. Images were recorded with light of 515/10 nm (1.3 W/cm$^2$) using an Alta CCD-camera (Apogee Instruments). For the statistical analysis, only cells expressing Dreiklang were considered.

**Single-molecule switching nanoscopy.** Single-molecule-switching imaging was performed on a home-built setup (**Supplementary Fig. 16**) that has been detailed before[39]. The nanoscope was equipped with continuous-wave lasers emitting at 488 nm (Ar-Kr laser Innova 70C-5, Coherent) for fluorescence excitation, at 355 nm (solid state, Zouk, Cobolt) for switching on and at 405 nm (laser diode, Oxxius; Laser2000) for switching off. Furthermore, it was equipped with an oil immersion objective lens (HCX PL APO 100×/1.4 oil, Leica) for creating an approximately (12 × 12) µm$^2$ large excitation spot and with a fast EMCCD camera (IXON-DU-897-CSO-BV, Andor Technology) for detection of fluorescence in epi-direction. The use of an EMCCD camera at high gain ensured that the read-out noise was negligible. The frame rate of the camera was optimized to minimize the background (100 Hz). The fluorescence was further cleaned by inserting a band pass filter (532/211; AHF Analysentechnik) to minimize the out-of-band background. Image acquisition, localization, spectral assignment, image reconstruction and simulations of two-dimensional histograms were performed as described before[41]. Image acquisition was started after switching off the protein ensemble in a preselected cell region until clear signatures of single emitters were observed. Switching of the lasers was controlled by a fast shutter (Uniblitz, Acal BFI Optilas) for the 491 nm laser, an acousto-optical modulator (AOM, AAA; Pegasus Optik) for the 355 nm laser and direct modulation of the 405 nm diode laser. Synchronization of the camera and the laser switching was realized by the IMSPECTOR software.

We defined the average number of photons $n_{fl}$ = 720 detected per single emitter by the expectation value of the geometrical distribution of photon counts per spots detected over the whole image-recording process. For the respective wide-field images, we simply added up the photons detected for all single-molecule events.

**RESOLFT imaging.** We modified a home-built confocal microscope (**Supplementary Fig. 17**). The microscope provided diffraction-limited foci of 355 nm (solid state, Zouk, Cobolt, for switching Dreiklang into the fluorescent state) and 491 nm laser light (solid state, Calypso, Cobolt, for probing the fluorescence of Dreiklang). A third laser path provided a doughnut-shaped focus at 405 nm (solid state, CrystaLaser) with a central intensity minimum for switching Dreiklang off at the focal periphery only. The 405 nm beam passed through a 2π phase ramp (407 nm mask, vortex plate VPP-1b, RPC Photonics) for creating a doughnut in the focal plane. A quarter and a half wave plate (B. Halle) were introduced in front of the objective for circularizing the polarization of all beams. Illumination powers and times were controlled by an acousto-optical-tunable filter (AOTF, AAA, Pegasus Optik) for the 491 nm and by acousto-optical modulators (AOM, AAA, Pegasus Optik) for the 405 and 355 nm light. Scanning of the probe was realized by a three-axis piezo table (NanoMax 311/M, Thorlabs). The experiment was synchronized by the IMSPECTOR software.

**Mass spectrometry.** For the determination of the molecular mass of the Dreiklang protein in its equilibrium, switched-off and switched-on states, 160 µg of the protein in 10 mM ammonium acetate buffer were diluted with or without prior photoswitching in 18% (vol/vol) acetonitrile/10 mM ammonium acetate. The photoswitching was done as described above.

ESI-MS analysis was performed under standard conditions on an LTQ-Orbitrap XL instrument (ThermoFisherScientific) in high-resolution mode (100,000) and on a Q-ToF ultima (Waters company) with infusion pump and static needle, respectively. Spectra were recorded and deconvoluted by using the manufacture's software tools (Excalibur and MaxEnd, respectively).

For the MALDI-ToF/ToF analysis, equilibrium-state Dreiklang was digested with trypsin (enzyme to substrate ratio, 1:20) at 37 °C overnight. Tryptic peptides were separated by nano liquid chromatography (LC), mixed with matrix, spotted onto MALDI target and analyzed by MALDI MS on a 4800 Proteome Analyser (ABSciex), as described previously[42]. MSMS spectra were annotated manually.

**Crystallographic analysis.** After purification, a Dreiklang protein solution was concentrated to ~35 µg/µl by ultrafiltration and taken up in 20 mM Tris/HCl, 120 mM NaCl, pH 7.5. The protein was crystallized by sitting drop vapor diffusion at 20 °C (293 K) with a reservoir solution containing 15% (wt/vol) PEG 3350, 0.2 M $KH_2PO_4$ and 3% (wt/vol) D-(+)-trehalose-dihydrate. The crystallization solution was cryoprotected by adding propane-1,3-diol to a final concentration of 25% (wt/vol).

For the structure determination of Dreiklang in the on- and the off-states, a single Dreiklang protein crystal was manually transferred into a vessel with

cryoprotected crystallization solution and then switched to the nonfluorescent state by irradiation with blue light (405 ± 10 nm, 110 W/cm$^2$) until the fluorescence signal reached a minimum. After switching the crystal, it was transferred within 10 s into liquid nitrogen, flash frozen, and diffraction data were collected at 100 K. Following the data collection of the off-state structure, the same crystal was unmounted, transferred back into cryoprotected crystallization solution kept at 25 °C and immediately switched to the fluorescent-state by irradiation with UV light (365 ± 25 nm, 1.4 W/cm$^2$) until the fluorescence signal reached a maximum. Subsequently the crystal was again flash frozen in liquid nitrogen and another diffraction data set was collected.

The equilibrium structure of Dreiklang was determined on crystals that have not been irradiated with light.

All diffraction data sets were collected on beamline 14-2 at BESSY (Berliner Elektronenspeicherring-Gesellschaft für Synchrotronstrahlung) using a MAR 225 mm CCD detector. Details for the refinement and crystallographic data are given in **Supplementary Table 2**. The data were processed using the XDS program package[43]. The crystal structures were solved by molecular replacement with PHASER[44] using the structure coordinates of Citrine (PDB ID 1HUY;[26]) as a model omitting the chromophore and the water molecules. The sequence was manually adjusted and fitted to the $2F_o–F_c$ and $F_o–F_c$ electron densities with COOT[45]. Atomic B-factors and coordinates were refined automatically with PHENIX.REFINE[46]. TLS (translation-libration-screw) refinement cycles were performed. Refinement was complemented by manual model building with COOT. Waters were built automatically with PHENIX.REFINE and completed manually. During the entire refinement procedure, 5% of randomly selected reflections were set aside for monitoring of the $R_{free}$ factor.

Finally, the omitted chromophore was placed manually into vacant patches of the $2F_o–F_c$ and $F_o–F_c$ electron densities. The chromophore restraints for the on-state fluorophore were generated with PRODRG[47], and the restraints of the off-state chromophore were generated with PHENIX.ELBOW[48].


38. Lamesch, P. *et al.* hORFeome v3.1: a resource of human open reading frames representing over 10,000 human genes. *Genomics* **89**, 307–315 (2007).
39. Testa, I. *et al.* Nanoscale separation of molecular species based on their rotational mobility. *Opt. Express* **16**, 21093–21104 (2008).
40. Patterson, G.H., Knobel, S.M., Sharif, W.D., Kain, S.R. & Piston, D.W. Use of the green fluorescent protein and its mutants in quantitative fluorescence microscopy. *Biophys. J.* **73**, 2782–2790 (1997).
41. Bossi, M. *et al.* Multicolor far-field fluorescence nanoscopy through isolated detection of distinct molecular species. *Nano Lett.* **8**, 2463–2468 (2008).
42. Richter, F.M., Sander, B., Golas, M.M., Stark, H. & Urlaub, H. Merging molecular electron microscopy and mass spectrometry by carbon film-assisted endoproteinase digestion. *Mol. Cell. Proteomics* **9**, 1729–1741 (2010).
43. Kabsch, W. Automatic processing of rotation diffraction data from crystals of initially unknown symmetry and cell constants. *J. Appl. Cryst.* **26**, 795–800 (1993).
44. McCoy, A.J. *et al.* Phaser crystallographic software. *J. Appl. Cryst.* **40**, 658–674 (2007).
45. Emsley, P. & Cowtan, K. Coot: model-building tools for molecular graphics. *Acta Crystallogr. D Biol. Crystallogr.* **60**, 2126–2132 (2004).
46. Adams, P.D. *et al.* PHENIX: a comprehensive Python-based system for macromolecular structure solution. *Acta Crystallogr. D Biol. Crystallogr.* **66**, 213–221 (2010).
47. Schuttelkopf, A.W. & van Aalten, D.M. PRODRG: a tool for high-throughput crystallography of protein-ligand complexes. *Acta Crystallogr. D Biol. Crystallogr.* **60**, 1355–1363 (2004).
48. Moriarty, N.W., Grosse-Kunstleve, R.W. & Adams, P.D. electronic ligand builder and optimization workbench (eLBOW): a tool for ligand coordinate and restraint generation. *Acta Crystallogr. D Biol. Crystallogr.* **65**, 1074–1080 (2009).





doi:10.1038/nbt.1952